RSC Advances

PAPER

View Article Online
View Journal | View Issue

Cite this: *RSC Adv.*, 2017, **7**, 38028

The effects of macromolecular crowding and surface charge on the properties of an immobilized enzyme: activity, thermal stability, catalytic efficiency and reusability†

Qiong Yang,[ab] Bochu Wang,*[a] Zhi Zhang,[a] Deshuai Lou,[c] Jun Tan[c] and Liancai Zhu[a]

The microenvironment around an immobilized enzyme molecule significantly influences the properties of the immobilized enzyme. To explore the combined effects of macromolecular crowding and surface charge on the properties of an immobilized enzyme, epoxy resin was modified by different quality percentage concentrations of chitosan to obtain different crowding and charge conditions of the microenvironment. With this system, the catalytic features of immobilized 7α- and 7β-hydroxysteroid dehydrogenase (7α-, 7β-HSDH) were investigated. The results indicate that the activities and thermal stabilities of immobilized 7α-HSDH and 7β-HSDH can be improved by manipulating the crowding and surface charge effects. The relative activity of immobilized 7α-HSDH and 7β-HSDH on EP-0.5-C increased approximately 90% and 50% relative to the immobilization onto EP. The immobilization of 7α-HSDH and 7β-HSDH onto EP-0.5-C preserved a higher activity (approximately 73% and 88% of the initial activity) than that preserved by immobilization onto EP (approximately 29% and 40% of the initial activity) after incubation at 45 °C for 2 h. In addition, the catalytic efficiency and reusability of co-immobilized 7α-HSDH and 7β-HSDH was improved. The TCDCA conversion of the co-immobilized enzymes onto EP-0.5-C was increased approximately 45%, compared to the conversion of the co-immobilized enzymes onto EP. The TCDCA conversion of the co-immobilized enzymes on EP-0.5-C remained at 83.72 ± 0.66% after seven successive cycles. These findings suggest that crowding and charge of the microenvironment can significantly improve the properties of the immobilized enzyme.

Received 12th June 2017
Accepted 25th July 2017

DOI: 10.1039/c7ra06544b

rsc.li/rsc-advances

1. Introduction

Enzymes are versatile and highly effective biological catalysts in the chemical, pharmaceutical, and food industries, deriving benefits from the environment and economies of scale.[1] Nevertheless, when enzymes are used in their native form, their activities may be hampered by such features as their low operational stability, high costs, and poor reutilization.[2] To overcome these barriers, enzyme immobilization has been routinely used with various supporting materials and different immobilization methods.[3–6] The microenvironment that surrounds an immobilized enzyme can be significantly changed when the free enzyme is immobilized on a solid carrier. Previous studies have shown that the microenvironment of an immobilized enzyme can determine the performance of the enzyme, with regards to its catalytic activity, stability, and selectivity.[7–9] In addition, macromolecular crowding and surface charge are important but neglected aspects of the enzyme microenvironment.

Up to 40% of the volume of the cytosol is well known to be occupied by a wide variety of macromolecules and solutes.[10] In recent years, the effects of crowding on enzyme activity have been investigated by various authors.[11,12] Macromolecular crowding has been shown to affect enzyme kinetics and enzymatic reaction initial velocities in solution. Likewise, macromolecular crowding may also affect the performance of immobilized enzymes on solid carriers. Kao *et al.* found that the α-helical domain was sensitive to protein denaturation in a crowded microenvironment using circular dichroism (CD) and fluorescence. The catalytic activity was enhanced mainly because of the crowding effect.[13] Liu *et al.* reported that the

[a]*Key Laboratory of Biorheological Science and Technology (Chongqing University), Ministry of Education, College of Bioengineering, Chongqing University, Chongqing 400030, PR China. E-mail: wangbc2000@126.com*

[b]*Chongqing Key Laboratory of Inorganic Special Functional Materials, Collaborative Innovation Center for Green Development in Wuling Mountain Areas, Yangtze Normal University, Chongqing 408100, PR China*

[c]*Chongqing Key Laboratory of Medicinal Resources in the Three Gorges Reservoir Region, School of Biological & Chemical Engineering, Chongqing University of Education, Chongqing 400067, PR China*

† Electronic supplementary information (ESI) available. See DOI: 10.1039/c7ra06544b

combined effects of macromolecular crowding on the performance of an immobilized enzyme was by accommodating lipase molecules into a series of mesoporous silicas with different amounts of inert poly(methacrylate) (PMA) covalently anchored inside the nanopores.[14] Likewise, the surface charge of immobilized enzyme carries is also a key factor in determining the properties of the enzymes. Studies have shown that the surface charge of the carrier can directly affect the configuration of an immobilized enzyme, the interaction between enzyme and carrier, and the degree to which the substrate is near the activity site of the enzyme molecule, which affects the catalytic efficiency of the immobilized enzyme.[15–17] From these initial findings, macromolecular crowding and surface charge should also be considered for their influence of immobilized enzymes.

Tauroursodeoxycholic acid (TUDCA) is widely used for treating human diseases.[18–20] The traditional strategy for preparing TUDCA is the chemical synthesis method. However, the complex process and by-products have limited its application. 7α-HSDH and 7β-HSDH have been exploited in the conversion of TCDCA to TUDCA (Fig. S1†).[21] To the best of our knowledge, no studies have reported on the macromolecular crowding effect or surface charge for improving the properties of immobilized 7α-HSDH and 7β-HSDH.

Epoxy resin and chitosan are commonly used as enzyme immobilization carriers, because of their many valuable chemical and biological properties.[22–25] Interestingly, we found that pore diameter and surface charge of immobilized enzyme carriers can be effectively adjusted by using different concentrations of chitosan in the modified epoxy resin. In addition, favorable conditions can be established for studying the effect of crowding and charge on the properties of immobilized enzymes.

In this work, we modified epoxy resin using different concentrations of chitosan, which allowed for adjustments in the degree of crowding and surface charge of the enzyme microenvironment. 7α-HSDH and 7β-HSDH were immobilized onto a series of carriers, and served as model enzymes. The activity and thermal stability of immobilized 7α-HSDH and 7β-HSDH were improved by changing the microenvironment. The catalytic efficiency and reusability were also improved with increased crowding and charge of the environment when both 7α-HSDH and 7β-HSDH were co-immobilized onto a series of carriers.

2. Methods

2.1. Materials

MC-150EP epoxy resin was purchased from Novocata Biotech Co. (Hangzhou, China). The chitosan flakes (95% deacetylated) used in the experiments were purchased from Sangon Biotech Co. (Shanghai, China). The expression and purification of 7α-HSDH (EC 1.1.1.159) and 7β-HSDH (EC 1.1.1.201) were performed using a GST gene fusion system.[26] TCDCA and TUDCA standard samples were purchased from the National Institutes for Food and Drug Control (Beijing, China). Sodium taurine-7-ketolithocholic acid (T-7-KLCA) was synthesized by our laboratory. β-$NADP^+$ (purity ≥ 95%) and NADPH (purity ≥ 95%) were purchased from Roche (Switzerland). The BCA protein assay reagent was purchased from Beyotime (Shanghai, China). Glutaraldehyde solution (concentration, 25%) was purchased from Kelong Chemicals (Chengdu, China). All other chemicals were analytical grade and used without further purification. Ultrapure water was used in all of the experiments.

2.2. Preparation of epoxy resin coated with chitosan

An appropriate amount of chitosan flakes was added to 100 mL of 2% (v/v) acetic acid solution under continuous stirring at 150 rpm and 25 °C for approximately 1 h. The gel was allowed to sit for 2 h to enable gas bubbles to escape. Next, 5 g of epoxy resin was added and stirred for 10 h at a stirring rate of 150 rpm at 25 °C. After removing excess chitosan solution with vacuum filtration, the epoxy resin with chitosan was dropped into 150 mL of 3% (w/v) sodium tripolyphosphate (STPP) and stirred for 3 h. The epoxy resin with chitosan was then removed from the STPP bath, and washed several times with ultrapure water until reaching a neutral pH and stored at 4 °C. The material was denoted as EP-*n*-C, where *n* (0.05, 0.1, 0.5, and 1) denotes the quality percentage concentration of chitosan in the modified epoxy resin.

2.3. Characterization methods

The chemical structure of the material was analyzed by FT-IR (5DX/550II, Nicolet, USA). Samples used for the FT-IR spectroscopic characterization were prepared by grinding the freeze-dried specimens with KBr and pressing them to form disks. Scanning electron microscope (SEM) images of the epoxy resin and the epoxy resin with chitosan were recorded with an SEM (EVOLS25, Zeiss, Germany). Confocal laser scanning microscope (CLSM) images were taken with a Leica TCS SP5 microscope (Leica, Wetzlar, Germany) at an excitation wavelength of 488 nm according to the FITC-labeled chitosan. The elemental analysis of the samples was performed with an elemental analyzer (Vario Macrocube, Germany). Nitrogen adsorption–desorption isotherm measurements were taken at 77 K with an ASAP2010 gas adsorption analyzer to determine the pore-size distribution of the carrier material. Pore-size distribution curves were made with the Barrett–Joyner–Halenda (BJH) method. The isoelectric point was determined by electrophoretic laser Doppler anemometry with a Zetasizer (NanoZS90, Malvern, UK). Samples were prepared in deionized water and sonicated for 15 min before the zeta potential was measured. The pH of the solution was manually adjusted by adding 0.1 M HCl or NaOH to 5–10 mL of the suspension before measuring the zeta potential. The water contact angle was measured to confirm the surface hydrophilicity of EP and EP-*n*-C. Samples were prepared by grinding the freeze-dried specimens and pressing them to form disks.

2.4. Immobilization of 7α-HSDH and 7β-HSDH

7α-HSDH and 7β-HSDH were purified and immobilized onto the EP-*n*-C as follows: approximately 0.5 g of EP-*n*-C was activated with glutaraldehyde solution (5 mL, 0.025%). The

activated EP-*n*-C (approximately 0.5 g) was suspended in 5 mL (1.2 mg mL^{-1}) of 7α-HSDH or 7β-HSDH solutions in phosphate buffer (50 mM, pH 7.2–7.4) and stirred at 150 rpm at 15 °C. After 4 h, the immobilized enzyme was washed three times in ultrapure water to remove unbound enzyme and then stored at 4 °C. The amount of 7α-HSDH or 7β-HSDH in the supernatant and washings was determined by the BCA protein assay reagent. The amount of 7α-HSDH or 7β-HSDH that was contained within the solid support was calculated from the difference in concentration of the enzyme solutions before and after immobilization.

The co-immobilization of 7α-HSDH and 7β-HSDH was performed as follows: 5 mL of the dual-enzyme solution (containing 2.5 mL (2.4 mg mL^{-1}) of 7β-HSDH and 2.5 mL (2.4 mg mL^{-1}) of 7α-HSDH) was added to about 0.5 g of the activated resin. After 4 h, the immobilized enzyme was washed three times in ultrapure water to remove unbound enzyme and then stored at 4 °C.

2.5. Activity assay, kinetic characterization and thermostability test

The 7α-HSDH (7β-HSDH) activity was measured for its catalytic conversion of TCDCA (TUDCA) by ultraviolet absorption of NADPH at 340 nm. The activity of immobilized 7α-HSDH (7β-HSDH) was determined in a total volume of 3 mL assay mixture containing 0.5 mM TUDCA, 0.2 mM $NADP^+$, and 0.5 g of immobilized enzyme. Next, the ultraviolet absorption of the supernatant was detected at 340 nm. The control test (without enzyme) was carried out with the same procedure and recorded as zero. In the biotransformation of TCDCA to TUDCA, coenzyme $NADP^+$ was reduced to NADPH.

In the kinetic studies of TCDCA conversion catalyzed by 7α-HSDH and TUDCA conversion catalyzed by 7β-HSDH, the reduction of $NADP^+$ was measured in the range of substrate concentrations from 0.25 to 10 mM, using UV-vis spectrophotometry. Kinetic parameters were calculated using the Michaelis–Menten equation.[27]

To test the thermostability of 7α-HSDH and 7β-HSDH, free 7α-HSDH (or 7β-HSDH) solution and immobilized 7α-HSDH (or 7β-HSDH) were incubated at a specific temperature (15 to 55 °C) in a thermostatically-controlled water bath for 2 h. The residual activity of the thermally-treated immobilized 7α-HSDH (or 7β-HSDH) was calculated by taking the initial activity, without thermal incubation (considered as being kept at 15 °C) as 100%.

2.6. Catalytic conversion of TCDCA using co-immobilized enzymes

Approximately 0.5 g of TCDCA was added to 100 mL of Tris–HCl buffer (50 mM, pH 8.5) and treated with ultrasound for 5 min (the stock solution). Then, 0.5 g of the co-immobilized enzymes, after being activated with a suitable amount of glutaraldehyde solution, and 0.4 mL of $NADP^+$ (50 mM) were mixed with 6 mL of TCDCA (6 mM) at a stirring rate of 150 rpm and incubated for 4 h. The solution was filtered to separate the immobilized dual-enzymes, which were then washed three times with Tris–HCl buffer (50 mM, pH 8.5). The products were freeze-dried before being used in the following experiments. TCDCA and TUDCA were evaluated by HPLC coupled with evaporative light-scattering detection (ELSD). The results were evaluated in terms of the conversion of TCDCA and the yield of TUDCA using the following equation.

$$\text{TCDCA conversion} = \frac{\text{the amount of TCDCA addition (mol)} - \text{the amount of TCDCA residues (mol)}}{\text{the amount of TCDCA addition (mol)}} \times 100\% \quad (1)$$

$$\text{TUDCA yield} = \frac{\text{the total amount of TUDCA (mol)}}{\text{the amount of TCDCA addition(mol)}} \times 100\% \quad (2)$$

Recycling experiments consisted of adding fresh TCDCA and $NADP^+$ to the co-immobilized enzymes every 7 cycles.

3. Results and discussion

3.1. Properties of 7α-HSDH and 7β-HSDH

For the immobilized enzymes, the performance of the free enzyme directly determines the performance of the immobilized enzyme. Therefore, the properties of 7α-HSDH and 7β-HSDH are important. The charge and surface properties of 7α-HSDH and 7β-HSDH (the structure of 7α-HSDH has been submitted to the Protein Data Bank (PDB code: 5EPO), while the structure of 7β-HSDH has not yet been submitted to the PDB) were examined by calculating the amino acid composition of the enzyme and their relative pK_a values (Fig. 1a and b). Based on the amino acid composition and the structure submitted to the PDB, ANTHEPROT 6.0 considers the shape and curvature of the enzyme molecule in its electrostatic potential calculations. Consequently, the charges of the enzyme at different pH values can be estimated. The specific method was as follows: enter the amino acid sequence of 7α-HSDH (GenBank: AET80685.1) and 7β-HSDH (GenBank: AET80684.1) into the ANTHEPROT 6.0, separately. Use the titration curve function to draw the isoelectric point. As our team has determined the crystal structure of 7α-HSDH and 7β-HSDH, we obtain the final structure in the PDB files. Open the PDB files for 7α-HSDH and 7β-HSDH with the PYMOL software and then perform the vacuum electrostatic action to generate the Poisson Boltzmann electrostatic surface potential of 7α-HSDH and 7β-HSDH. The calculated isoelectric point (pH_i) for 7α-HSDH and 7β-HSDH were 5.635 and 5.575, respectively (Fig. 1a and b). The protein net charge was calculated based on the pK_a values for the individual amino acids, and Poisson Boltzmann electrostatic potential calculations were performed within the PYMOL program (Fig. 1c and d). The electrostatic calculations for the surface of 7α-HSDH and 7β-HSDH indicate that the surface is negatively charged at pH 7, which is

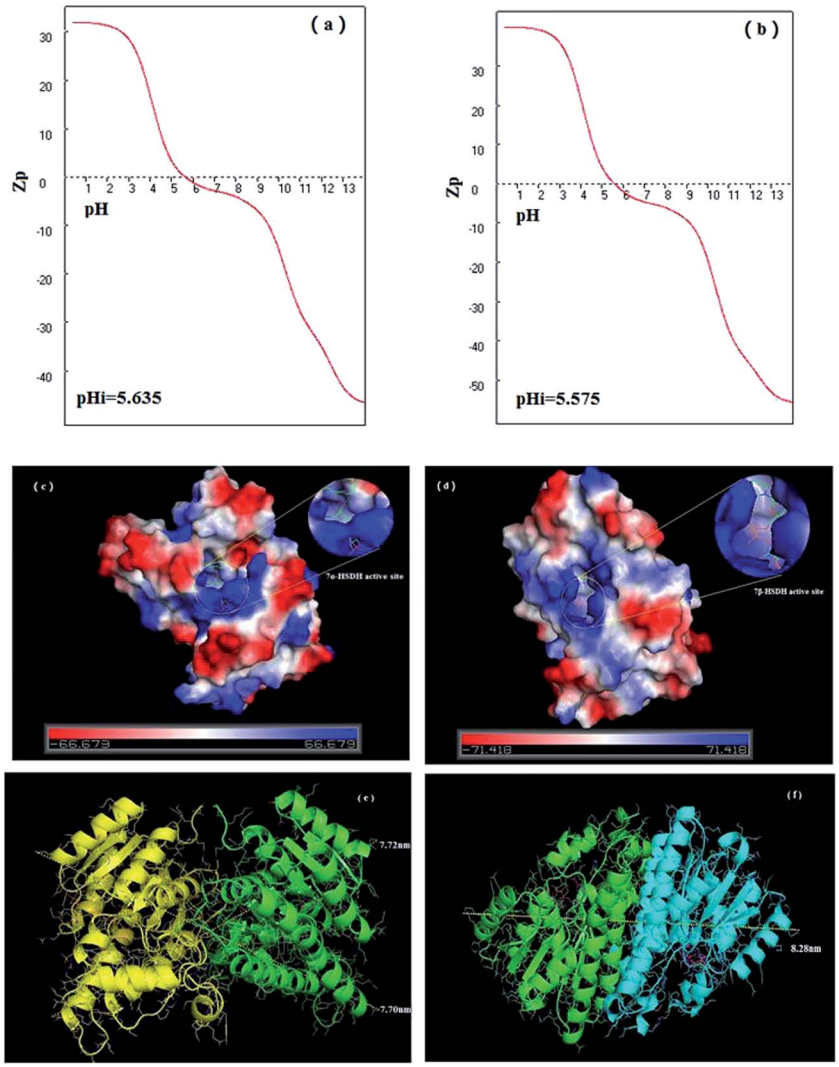

Fig. 1 Calculated charge of 7α-HSDH (a) and 7β-HSDH (b) as a function of pH and Poisson Boltzmann electrostatic surface potential of 7α-HSDH (c) and 7β-HSDH (d) as calculated in PYMOL at pH 7.0 (blue represents areas of positive charge and red represents areas of negative charge). The size of 7α-HSDH (e) and 7β-HSDH (f).

consistent with the isoelectric point (pH_i) of the protein. Interestingly, the active sites of 7α-HSDH and 7β-HSDH are predominantly positively charged.

Size exclusion chromatography (SEC) was used to determine the molecular weight distribution and the results indicate that in the CA, 7α-HSDH mainly exists as a dimer.[26] Therefore, the widest dimensions of 7α-HSDH and 7β-HSDH were calculated by the farthest distance between two amino acids with 7α-HSDH and 7β-HSDH existing as dimers (Fig. 1e and f). The results indicate that the widest dimensions of 7α-HSDH and 7β-HSDH were approximately 7.7 nm and 8.3 nm, respectively. This experiment suggests that if 7α-HSDH and 7β-HSDH were immobilized on a porous material with pore entrances greater than 8.3 nm, 7α-HSDH and 7β-HSDH could enter into the inner holes of the porous material.

3.2. Chitosan modified epoxy resin and its characterization

Epoxy resin has an active group (epoxy group), which has a high reaction activity and plasticity, so that it can react with many groups, such as amino, hydroxyl, imidazole, or carboxyl.[28] Meanwhile, chitosan is rich in amino groups and has been widely studied as an excellent enzyme carrier.[24,29] Epoxy resin could theoretically be modified with chitosan to take advantage of the properties of epoxy resin and chitosan. EP-0.5-C was measured to determine whether or not the modification was successful.

The FT-IR spectra of chitosan, epoxy resin, and EP-0.5-C are compared in Fig. S2.† The bands at about 3400 cm^{-1} and 1642 cm^{-1} were characteristic vibration absorptions for N–H on the surface of the chitosan and EP-0.5-C. The experiment revealed that the epoxy resin could be successfully modified with chitosan.

The elemental analysis showed that the composition of the epoxy resin was 59.69% (C), 6.6% (H), 0.073% (N), and 0.618% (S), whereas the composition of EP-0.5-C was 58.17% (C), 6.519% (H), 0.315% (N), and 0.457% (S). The low concentration of nitrogen in the epoxy resin was due to the interference of nitrogen in the air, while its higher concentration in EP-0.5-C was due to presence of chitosan.

The morphology of the epoxy resin and EP-0.5-C was analyzed by SEM (Fig. S3†). The SEM images of epoxy resin (Fig. S3a†) indicate that the average size of the microbeads of epoxy resin was 150–270 μm, and they appeared to be spherical and uniform. Fig. S3b† is a magnified image of Fig. S3a,† clearly showing the uniform pores, which are suitable for immobilizing the enzyme. Fig. S3c and d† show the chitosan coating on the exterior of the epoxy resin microbeads.

To confirm that the epoxy resin had been successfully modified with chitosan, the epoxy resin microbeads were coated with FITC fluorescein-labeled chitosan for fluorescence imaging and confocal laser scanning microscopy (CLSM) imaging. Fig. S4a† shows fluorescence images of the FITC fluorescein-labeled chitosan coated epoxy resin. The chitosan coating could also be seen on the exterior of the epoxy resin microbeads. Fig. S4b† shows images from CLSM of the FITC fluorescein-labeled, chitosan coated epoxy resin. The results show that the distribution profiles of chitosan within the microbeads is highly dependent on pore size. Thus, chitosan could successfully modify the epoxy resin not only by coating the exterior of the epoxy resin microbeads, but also by entering into the microbeads.

3.3. Physicochemical properties of EP-*n*-C

From the SEM analysis, epoxy resin and EP-0.5-C have uniform porous structures. The BET surface area (S_{BET}), pore diameter (D_{BJH}), and total pore volume (V_p) of EP-*n*-C all decrease with increasing quality percentage concentrations of chitosan within the samples (Table 1), presumably owing to the occupation of pore spaces by chitosan. EP and EP-*n*-C exhibit large pore openings (approximately 18–31 nm) that should easily allow 7α-HSDH and 7β-HSDH (approximately 7.7 nm and 8.3 nm, respectively) to enter the mesoporous channels (Fig. 1e and f). The decreasing pore diameters (D_{BJH}) also provides an opportunity for investigating the macromolecular crowding effect for immobilized enzymes.

The surface hydrophobicity of EP-*n*-C was investigated by the water contact angle of EP-*n*-C. The results reveal that the surface hydrophobicity of EP-*n*-C increases with increasing quality percentage concentrations of chitosan (Table 1). Nevertheless, the water contact angle only increased slightly (from 43.4 ± 2.1° to 48.7 ± 2.3°) from EP to EP-1-C. Thus, these results suggest that the surface hydrophobicity of EP-*n*-C is not the main reason for the loading and activity of the enzyme.

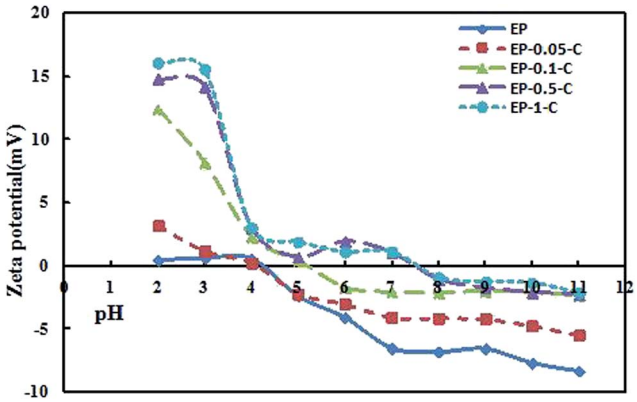

Fig. 2 Zeta potential as a function of pH for EP and EP-*n*-C.

From Fig. 2, the zeta potential of EP and EP-0.05-C as a function of PH yields an isoelectric point of 4.3. The isoelectric point increases with the increasing concentration of the modified chitosan. The isoelectric point of EP-0.5-C and EP-1-C were about pH 7.4 (pH 7.2–7.4) in PBS, a commonly used buffer. Previous studies have shown that immobilized 7α-HSDH and 7β-HSDH have higher loading and activity in PBS buffer (pH 7.2–7.4). At pH 7.4, EP-0.5-C and EP-1-C are almost without charge, and EP, EP-0.05-C, and EP-0.1-C have varying degrees of negative charge.

3.4. Activity of 7α-HSDH and 7β-HSDH immobilized onto EP-*n*-C

To examine whether or not the activity of immobilized enzyme is influenced by the microenvironment, in terms of crowding and charge, 7α-HSDH and 7β-HSDH were immobilized onto EP and EP-0.05-C, respectively, in PBS (pH 7.2–7.4). The EP was pretreated by washing three times with ultrapure water and then ultrafiltered until dry, and the EP-*n*-C was activated with glutaraldehyde solution (0.025%). The loading of 7β-HSDH ($L_{7\beta\text{-HSDH}}$) was markedly lower than that of 7α-HSDH ($L_{7\alpha\text{-HSDH}}$) under similar conditions (Table 1), presumably due to the greater net charge of 7β-HSDH (−5.3), compared to 7α-HSDH (−3.2) at pH 7.2–7.4. EP and EP-*n*-C have varying degrees of negative charge, which creates more difficulty for the 7β-HSDH to close the carrier in the cross-linking reaction. The loading of 7α-HSDH ($L_{7\alpha\text{-HSDH}}$) is slightly different for EP and EP-*n*-C (10.29 ± 0.30 to 10.46 ± 0.21 mg g^{-1}), and the loading of 7β-HSDH ($L_{7\beta\text{-}}$

Table 1 Textural parameters of carriers and the loading of 7α- and 7β-HSDH, and surface hydrophobic properties[a]

Sample	D_{BJH} (nm)	S_{BET} (m^2 g^{-1})	V_p (cm^3 g^{-1})	$L_{7\alpha}$ (mg g^{-1})	$L_{7\beta}$ (mg g^{-1})	Average (°)
EP-1-C	18.46	97.53	0.32	10.46 ± 0.21	9.22 ± 0.31	48.7 ± 2.3
EP-0.5-C	18.53	98.31	0.33	10.41 ± 0.19	9.21 ± 0.15	48.4 ± 2.1
EP-0.1-C	20.37	98.37	0.33	10.31 ± 0.26	9.29 ± 0.21	47.1 ± 1.9
EP-0.05-C	28.35	99.53	0.34	10.35 ± 0.14	9.12 ± 0.28	45.3 ± 2.1
EP	30.48	100.76	0.35	10.29 ± 0.30	9.17 ± 0.32	43.4 ± 2.1

[a] D_{BJH}, S_{BET}, and V_p refer to the pore diameter, BET surface area, and total pore volume. $L_{7\alpha}$ and $L_{7\beta}$ are the loading of 7α- and 7β-HSDH. Average is the water contact angle of EP-*n*-C.

$_{HSDH}$) has the same experimental results (9.17 ± 0.32 to 9.22 ± 0.31 mg g^{-1}). The pore diameters of EP and EP-*n*-C (31 to 18 nm) were sufficiently large to allow the 7α-HSDH and 7β-HSDH (approximately 7.7 nm and 8.3 nm, respectively) molecules to enter the mesoporous channels. The pore diameters of EP and EP-*n*-C decrease with increasing concentrations of chitosan, indicating an increasing degree of crowding in the immobilized enzyme systems within pores with higher concentrations of chitosan.

The activities of immobilized 7α-HSDH and 7β-HSDH were measured by changes in UV-absorption from the reduction of $NADP^+$ to NADPH in the conversion of TCDCA to TUDCA. The highest enzyme activity was defined as 100%.

The relative activities of the immobilized enzymes were calculated as shown in Fig. 3.

The results indicate the highest activity when 7α-HSDH and 7β-HSDH were immobilized onto EP-0.5-C under similar conditions. The relative activities of immobilized 7α-HSDH and 7β-HSDH onto EP were 9.6% and 48.7%, respectively. For EP that was modified with chitosan, the relative activities gradually increased until reaching the maximum relative activity (100%), which was achieved by 7α-HSDH and 7β-HSDH immobilized onto EP-0.5-C. The next highest relative activities (93% and 98%) were achieved by 7α-HSDH and 7β-HSDH immobilized onto EP-1-C. Two possible explanations may be given for the change in immobilized enzyme activity. On the one hand, at pH 7.2–7.4, EP-0.5-C and EP-1-C are almost without charge. EP, EP-0.05-C, and EP-0.1-C have varying degrees of negative charge. Although 7α-HSDH and 7β-HSDH are negatively charged at pH 7.2–7.4, the microenvironments at the enzyme active centers are positively charged. During the immobilization, the active sites of 7α-HSDH and 7β-HSDH are attracted by an electrostatic force with EP, EP-0.05-C, and EP-0.1-C, so that their active sites that are close to the carrier would block the enzyme active site, and reduce the possibility of substrate being near the enzyme active site. At the same time, the active sites of 7α-HSDH and 7β-HSDH were not affected since EP-0.5-C and EP-1-C carried no net charge. Consequently, the relative activities of the two enzymes immobilized onto EP-*n*-C ($n = 0.5, 1$) were higher than those of 7α-HSDH and 7β-HSDH immobilized onto EP and EP-*n*-C ($n = 0.05, 0.1$) (Fig. 3). On the other hand, the degree of crowding in immobilized enzyme systems within the pores increases with increasing concentrations of chitosan. This increase in enzyme activity has been widely reported to be due to macromolecular crowding.[30–32] It is reasonable to presume that the macromolecular crowding effect may play a significant part in improving the enzyme activity of immobilized 7α-HSDH and 7β-HSDH.

Table 2 Kinetic parameters of 7α-HSDH and 7β-HSDH

Enzyme	Substrate	V_{max} (μmol min^{-1})	K_m (mM)
Free 7α-HSDH	TCDCA	21.45	0.23
Free 7β-HSDH	TUDCA	51.60	1.12
EP-7α-HSDH	TCDCA	0.015	0.91
EP-0.05-C–7α-HSDH	TCDCA	0.035	0.88
EP-0.1-C–7α-HSDH	TCDCA	0.04	0.64
EP-0.5-C–7α-HSDH	TCDCA	0.10	0.38
EP-1-C–7α-HSDH	TCDCA	0.12	0.39
EP-7β-HSDH	TUDCA	0.28	0.35
EP-0.05-C–7β-HSDH	TUDCA	0.36	0.34
EP-0.1-C–7β-HSDH	TUDCA	0.42	0.32
EP-0.5-C–7β-HSDH	TUDCA	0.57	0.31
EP-1-C–7β-HSDH	TUDCA	0.57	0.32

The Michaelis–Menten kinetics of free HSDH and immobilized HSDH were also studied (Table 2). In Table 2, with the increasing degree of crowding around the immobilized enzyme, the corresponding K_m values of the immobilized 7α-HSDH and 7β-HSDH show a decreasing trend. This reflects an enhanced affinity between the active sites of the enzyme and the substrate molecules. Jiang reported that, in protein solution systems, macromolecular crowding could improve the intrinsic catalytic efficiency of an enzyme by enhancing its affinity for the substrates, as seen with the decrease in the Michaelis–Menten constant (K_m).[33] This could also contribute to the increased enzyme activity in our system.

3.5. Stability of 7α-HSDH and 7β-HSDH immobilized onto EP-*n*-C

The thermal stability of free 7α-HSDH and 7β-HSDH and the immobilized enzymes was evaluated by measuring their residual activities at 25 °C after being incubated for 2 h at an elevated temperature (15–55 °C). The results are shown in Fig. 4. Obviously, the thermal stability of immobilized 7α-HSDH and 7β-HSDH was better than the thermal stability of the free

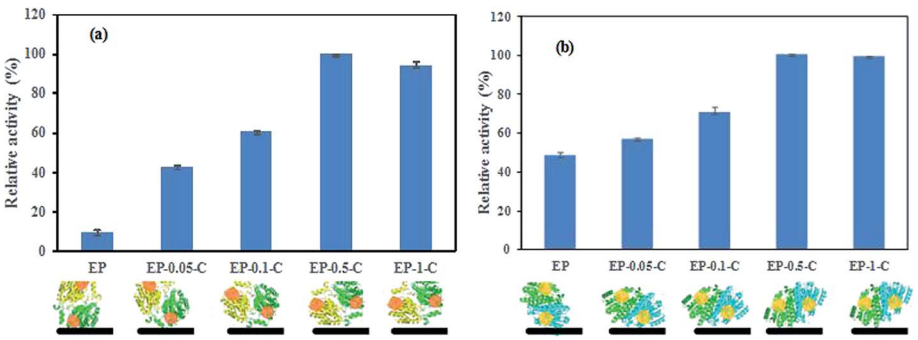

Fig. 3 Relative activities of 7α-HSDH (a) and 7β-HSDH (b) immobilized onto EP and EP-*n*-C, and the schematic illustration of active site close to the carrier.

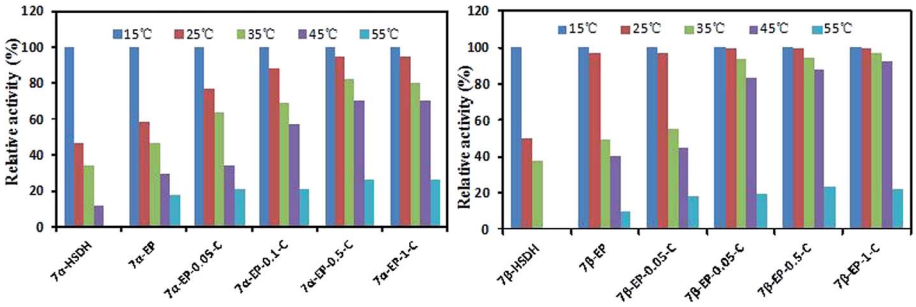

Fig. 4 Residual activities of 7α-HSDH and 7β-HSDH immobilized onto EP and EP-*n*-C after incubation for 2 h at different temperatures.

enzymes. Free 7α-HSDH and 7β-HSDH were highly sensitive to temperature and a significant decline in activity was seen when incubation was at 25 °C. The relative activities of 7α-HSDH and 7β-HSDH were 46.47% and 50.34%, respectively. The activities of free 7α-HSDH and 7β-HSDH were hardly detectable when they were treated at 45 °C for 2 h. As an explanation, after the enzyme was immobilized on the carrier, the rigidity of the enzyme domain structures is strengthened and the flexibility of the enzyme is weakened. External forces are smaller in influencing the enzyme configuration; thus, the thermal stability of the immobilized 7α-HSDH and 7β-HSDH is greater than that of the free enzymes. Immobilized 7α-HSDH and 7β-HSDH onto EP showed better thermal stability than the free enzymes, but the activity still decreased with increasing temperature. When 7β-HSDH was immobilized onto EP-0.5-C, no remarkable loss in activity was detected over the temperature range (15–45 °C) and 88.35% activity was retained, even after incubation at 45 °C. With 7α-HSDH immobilized onto the EP-*n*-C, the thermal stability in the temperature range (15–45 °C) was enhanced with increasing concentrations of chitosan. All immobilized enzymes had lower activities after the thermal treatment for 2 h at 55 °C, indicating that immobilized 7α-HSDH and 7β-HSDH are unsuitable for use at temperatures above 55 °C. Many studies have shown that a crowded microenvironment around an enzyme is conducive to their thermal stability, mainly due to the crowding effect that can shift the equilibrium in favor of the more-compact native (folded) state of the enzyme.[32,34,35] An equilibrium statistical-thermodynamic model primarily developed from Minton predicts that macromolecular crowding should increase a protein's thermal stability (T_m) by a magnitude of 5–20 °C under physiological solute conditions.[36] The pore diameter (D_{BJH}) of EP-*n*-C was changed to a large extent (30–18 nm) by different concentrations of chitosan in the modified epoxy resin, and to a slight extent by the surface hydrophobic properties. In our case, macromolecular crowding and the thermal stability of the immobilized 7α-HSDH and 7β-HSDH have a close relationship. The epoxy resin modified with different concentrations of chitosan is preferred for improving the thermal stability of immobilized 7α-HSDH and 7β-HSDH.

3.6. Catalytic efficiency and reusability of co-immobilized 7α-HSDH and 7β-HSDH

The activity and thermal stability of 7α-HSDH and 7β-HSDH immobilized on EP and EP-*n*-C were investigated in the previous experiments. The results show that the activity and thermal stability of the immobilized 7α-HSDH and 7β-HSDH increase with the concentration of chitosan, to various degrees. Nevertheless, the synthesis of TUDCA requires multi-step reactions by 7α-HSDH and 7β-HSDH, and a single immobilized enzyme does not satisfy the demands for the reaction. In addition, our experiments show that the co-immobilized 7α-HSDH and 7β-HSDH have higher TCDCA conversions and TUDCA yields, when compared to simple mixtures of immobilized 7α-HSDH and 7β-HSDH for the catalytic conversion of TCDCA.[21] Therefore, we co-immobilized 7α-HSDH and 7β-HSDH on EP and EP-*n*-C (n = 0.05, 0.1, 0.5, 1) to explore the influence of macromolecular crowding and surface charge on the catalytic conversion of TCDCA and enzyme reusability.

The results of catalytic conversion of TCDCA using the dual enzyme co-immobilization on different carriers are shown in Table 3. Immobilized dual-enzymes on EP displayed the lowest TCDCA conversions and TUDCA yields of 39.8 ± 1.84% and 14.48 ± 0.14%, respectively. The conversion of TCDCA and the yield of TUDCA are greatly improved with increasing concentrations of chitosan. When 7α-HSDH and 7β-HSDH were co-immobilized on EP-0.5-C and EP-1-C, the conversion of TCDCA was 85.45 ± 0.36% and 85.47 ± 0.46%, respectively, and the yield of TUDCA was 55.03 ± 2.01% and 55.12 ± 0.17%, respectively. These results are consistent with the activity of single, immobilized 7α-HSDH and 7β-HSDH. This indicates that the macromolecular crowding and surface charge improved the activity of immobilized enzyme, which in turn, improved the catalytic efficiency of the immobilized enzyme.

The reusability of immobilized enzymes is an important index for evaluating the performance of immobilized enzymes in specific applications. The effect of macromolecular crowding around an immobilized enzyme can also influence the reusability of the immobilized dual-enzymes in catalytic

Table 3 The catalytic conversion TCDCA results using co-immobilized 7α- and 7β-HSDH on different carriers

Carrier	TUDCA yield (%)	TCDCA conversion (%)
EP	14.48 ± 0.14	39.8 ± 1.84
EP-0.05-C	41.03 ± 2.57	69.12 ± 0.35
EP-0.01-C	48.66 ± 0.12	80.17 ± 0.27
EP-0.5-C	55.03 ± 2.01	85.45 ± 0.36
EP-1-C	55.12 ± 0.17	85.47 ± 0.46

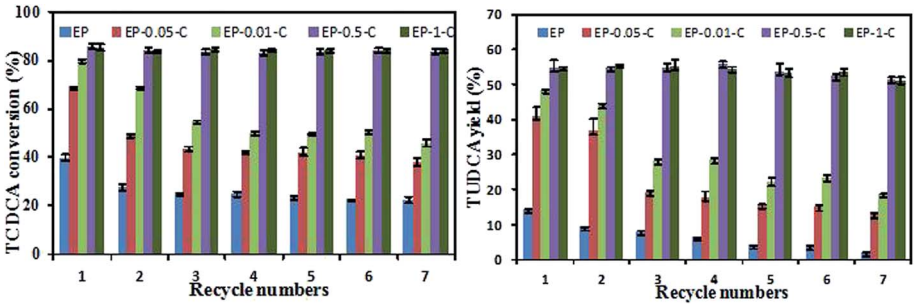

Fig. 5 Reusability of co-immobilized 7α- and 7β-HSDH on different carriers for TCDCA conversion.

conversions of TCDCA (Fig. 5). The conversion of TCDCA by an enzyme that is co-immobilized on EP presents an apparent decrease from 39.8 ± 1.84% to 22.33 ± 1.59%, and a decreased yield of TUDCA from 14.48 ± 0.14% to 2.1 ± 0.2% after seven successive cycles. When the dual-enzymes are immobilized on EP-0.5-C and EP-1-C, the TCDCA conversion is still 83.72 ± 0.66% and 84.32 ± 0.55%, respectively, and the TUDCA yield is 51.54 ± 0.67% and 51.14 ± 0.95%, respectively. These results clearly demonstrate that EP-*n*-C has greater recycling stability, compared to EP. The reusability of the immobilized dual-enzymes on EP-*n*-C is better with the crowded microenvironment of the immobilization enzyme systems inside the pores, with increasing concentrations of chitosan. The reusability of the immobilized enzymes can thus be improved with the crowded microenvironment.

4. Conclusions

In summary, a series of new carriers were produced by using different quality percentage concentrations of chitosan to modify epoxy resin. Nitrogen adsorption–desorption isotherms and isoelectric points of the series of carriers demonstrated that the crowding effect and charge of the immobilized enzyme microenvironments were altered by the different concentrations of chitosan. Although a series of carriers had similar loading capacities, the increased crowding and charge of the enzyme environment can improve the properties of the immobilized 7α-HSDH and 7β-HSDH, in terms of activity and thermal stability. When 7α-HSDH and 7β-HSDH were co-immobilized on EP and EP-*n*-C, the catalytic efficiency and reusability were improved with increased crowding and charge of the enzyme environments. Our findings suggest that crowding and charge of the immobilized enzyme microenvironment play a significant part in improving the properties of the immobilized enzymes. Our experiments also provide a novel approach for creating more efficient carriers for immobilized enzymes in industrial applications.

Acknowledgements

This work was supported by the National Science and Technology Major Projects for "Major New Drugs Innovation and Development" (2014ZX09301306-007), and the Scientific and Technological Research Program of Chongqing Municipal Education Commission (KJ1601216).

References

1 H. E. Schoemaker, D. Mink and M. G. Wubbolts, *Science*, 2003, **299**, 1694–1697.
2 U. T. Bornscheuer, *Angew. Chem., Int. Ed. Engl.*, 2003, **42**, 3336–3337.
3 A. Mukhopadhyay, A. K. Dasgupta and K. Chakrabarti, *Bioresour. Technol.*, 2015, **179**, 573–584.
4 J. Rocha-Martin, A. Acosta, J. Berenguer, J. M. Guisan and F. Lopez-Gallego, *Bioresour. Technol.*, 2014, **170**, 445–453.
5 I. S. Tan and K. T. Lee, *Bioresour. Technol.*, 2015, **184**, 386–394.
6 E. Yilmaz, K. Can, M. Sezgin and M. Yilmaz, *Bioresour. Technol.*, 2011, **102**, 499–506.
7 T. L. Klotzbach, M. Watt, Y. Ansari and S. D. Minteer, *J. Membr. Sci.*, 2008, **311**, 81–88.
8 G. Bayramoglu, B. Altintas, M. Yilmaz and M. Y. Arica, *Bioresour. Technol.*, 2011, **102**, 475–482.
9 S. Engel, H. Hock, M. Bocola, H. Keul, U. Schwaneberg and M. Moller, *Polymer*, 2016, **8**, 16.
10 R. J. Ellis, *Curr. Opin. Struct. Biol.*, 2001, **11**, 500.
11 I. Pastor, L. Pitulice, C. Balcells, E. Vilaseca, S. Madurga, A. Isvoran, M. Cascante and F. Mas, *Biophys. Chem.*, 2014, **185**, 8–13.
12 C. Balcells, I. Pastor, E. Vilaseca, S. Madurga, M. Cascante and F. Mas, *J. Phys. Chem. B*, 2014, **118**, 4062–4068.
13 K.-C. Kao, T.-S. Lin and C.-Y. Mou, *J. Phys. Chem. C*, 2014, **118**, 6734–6743.
14 J. Liu, J. Peng, S. Shen, Q. Jin, C. Li and Q. Yang, *Chemistry*, 2013, **19**, 2711–2719.
15 S. Hudson, J. Cooney, B. K. Hodnett and E. Magner, *Chem. Mater.*, 2007, **19**, 2049–2055.
16 C. H. Lee, J. Lang, C. W. Yen, P. C. Shih, T. S. Lin and C. Y. Mou, *J. Phys. Chem. B*, 2005, **109**, 12277–12286.
17 A. Vinu, V. Murugesan, O. Tangermann and M. Hartmann, *Chem. Mater.*, 2004, **16**, 3056–3065.
18 S. Caglieris, E. Giannini, G. Dardano, L. Mondello, U. Valente and R. Testa, *Hepato-Gastroenterology*, 2000, **47**, 1045–1047.
19 E. J. Cho, J. H. Yoon, M. S. Kwak, E. S. Jang, J. H. Lee, S. J. Yu, Y. J. Kim, C. Y. Kim and H. S. Lee, *Dig. Dis. Sci.*, 2014, **59**, 1461–1474.
20 D. Laukens, L. Devisscher, L. Van den Bossche, P. Hindryckx, R. E. Vandenbroucke, Y.-P. Vandewynckel, C. Cuvelier,

B. M. Brinkman, C. Libert, P. Vandenabeele and M. De Vos, *Lab. Invest.*, 2014, **94**, 1419–1430.
21 Q. Ji, J. Tan, L. Zhu, D. Lou and B. Wang, *Biochem. Eng. J.*, 2016, **105**, 1–9.
22 D. Jung, C. Streb and M. Hartmann, *Int. J. Mol. Sci.*, 2010, **11**, 762–778.
23 Preety and V. Hooda, *Appl. Biochem. Biotechnol.*, 2014, **172**, 115–130.
24 B. Krajewska, *Enzyme Microb. Technol.*, 2004, **35**, 126–139.
25 E. Skoronski, M. Fernandes, M. d. L. Borba Magalhaes, G. F. da Silva, J. J. Joao, C. H. Lemos Soares and A. Furigo Junior, *Molecules*, 2014, **19**, 16794–16809.
26 D. Lou, B. Wang, J. Tan, L. Zhu, X. Cen, Q. Ji and Y. Wang, *Sci. Rep.*, 2016, **6**, 22885.
27 D.-M. Liu, J. Chen and Y.-P. Shi, *RSC Adv.*, 2015, **5**, 56841–56847.
28 J. Turková, K. Bláha, M. Malaníková, D. Vančurová, F. Švec and J. Kálal, *Biochim. Biophys. Acta*, 1978, **524**, 162–169.
29 E. Skoronski, M. Fernandes, L. Magalhaes Mde, G. F. da Silva, J. J. Joao, C. H. Soares and A. F. Junior, *Molecules*, 2014, **19**, 16794–16809.
30 R. J. Ellis and A. P. Minton, *Nature*, 2003, **425**, 27–28.
31 X. Q. Wang, D. N. Lu, R. Austin, A. Agarwal, L. J. Mueller, Z. Liu, J. Z. Wu and P. Y. Feng, *Langmuir*, 2007, **23**, 5735–5739.
32 A. Wang, C. Zhou, Z. Du, M. Liu, S. Zhu, S. Shen and P. Ouyang, *J. Biosci. Bioeng.*, 2009, **107**, 219–224.
33 M. Jiang and Z. Guo, *J. Am. Chem. Soc.*, 2007, **129**, 730–731.
34 Y. Wang, H. He and S. Li, *Biochemistry*, 2010, **75**, 648–654.
35 J. Jia, X. Peng, W. Qi, R. Su and Z. He, *Int. J. Biol. Macromol.*, 2017, **101**, 373–382.
36 A. P. Minton, *Biophys. J.*, 2000, **78**, 101–109.